Letter

Sign-tunable exchange bias effect in proton-intercalated Fe_3GaTe_2 nanoflakes

Chunsheng Wang,[1,2,*] Jie Wang,[2,*] Wen-Qiang Xie,[3,4,*] Gaojie Zhang,[5,6] Hao Wu,[5,6] Jianhui Zhou,[2] Xiangde Zhu,[2] Wei Ning,[2] Guopeng Wang,[1] Cheng Tan,[7] Lan Wang,[7] Haifeng Du,[2] Yu-Jun Zhao,[4,†] Haixing Chang,[5,6,8,‡] Guolin Zheng,[2,§] Wen-Tong Geng,[3] and Mingliang Tian[1,2]

[1]*School of Physics and Optoelectronic Engineering, Anhui University, Hefei 230601, Anhui, China*
[2]*Anhui Province Key Laboratory of Condensed Matter Physics at Extreme Conditions, High Magnetic Field Laboratory, Chinese Academy of Sciences (CAS), Hefei 230031, Anhui, China*
[3]*School of Materials Science and Engineering, Hainan University, Haikou 570228, China*
[4]*Department of Physics, South China University of Technology, Guangzhou 510640, China*
[5]*Center for Joining and Electronic Packaging, State Key Laboratory of Material Processing and Die and Mold Technology, School of Materials Science and Engineering, Huazhong University of Science and Technology, Wuhan 430074, China*
[6]*Wuhan National High Magnetic Field Center and Institute for Quantum Science and Engineering, Huazhong University of Science and Technology, Wuhan 430074, China*
[7]*School of Science, RMIT University, Melbourne, VIC 3001, Australia*
[8]*Shenzhen R&D Center of Huazhong University of Science and Technology (HUST), Shenzhen 518000, China*

(Received 18 December 2022; accepted 30 March 2023; published 20 April 2023)

The exchange-bias (EB) effect, usually arising in ferromagnetic (FM)-antiferromagnetic (AFM) interfaces with uniaxial magnetic anisotropy, holds high potentials in spintronic applications. Here, we report both field-cooling and zero-field cooling EB effects with a maximal EB field $|H_{EB}|$ reaches up to 3859 Oe in above-room-temperature van der Waals (vdW) ferromagnet Fe_3GaTe_2 nanoflakes at low temperatures. The observed intrinsic EB effects can be largely tuned via the gate-induced proton intercalation. Moreover, we observe an unusual sign-tunable EB effect under different gate voltages after ± 2 T field cooling, leading to a crossover between positive and negative EB effects. Theoretical analysis based on density functional theory indicates that the magnetic coupling at the FM/AFM interface in proton-intercalated Fe_3GaTe_2 is highly controllable and can be tuned to be FMI-1 ($\uparrow$ / $\downarrow\uparrow$, positive EB) or FMI-2 ($\downarrow$ / $\downarrow\uparrow$, negative EB) magnetic configurations, depending on different H-absorption sites. Our experiments offer a knob to control the sign of EB effects and further open opportunities for more applicable spintronic devices in high-temperature vdW ferromagnets.

DOI: 10.1103/PhysRevB.107.L140409

Searching for van der Waals (vdW) magnets [1–7] and constructing relevant vdW spintronic devices [8–22] have opened a new arena of research in physics and materials science. Among them, iron-based vdW ferromagnets Fe_xGeTe_2 ($x = 3$–5) [3,5–7] are of special interest due to their high Curie temperatures and vast potentials in spintronic applications. Recently, another iron-based vdW ferromagnet Fe_3GaTe_2 (FGaT) was found to be an above-room-temperature ferromagnet ($T_c \sim 340$ K in bulk) with very large perpendicular magnetic anisotropy (with perpendicular magnetic anisotropy energy density $\sim 4.79 \times 10^5 \mathrm{J/m^3}$) and large anomalous Hall angle (3%) at room temperature [23]. FGaT has, thus, become one of the ideal platforms to develop the room-temperature vdW spintronic devices. However, the magnetic properties in this intriguing material especially with charge doping are not fully resolved.

Here, we report huge field-cooling (FC) and zero-field cooling (ZFC) exchange bias (EB) effects in FGaT nanoflakes with the maximal FC EB field $|H_{EB}|$ reaches up to 3859 Oe. The FC EB effect in intrinsic FGaT nanoflakes can be either positive or negative, revealing different magnetic coupling types in FM/AFM interfaces. Under a protonic gate, however, we found the sign of the FC EB effect can be *in situly* tuned via the gate-induced proton intercalation, leading to a crossover between positive and negative EB effects. Besides the FC EB effects, ZFC EB effects were found suppressed and finally disappeared whereas sweeping the gate voltage up to -6.5 V. These observations can be well captured by theoretical analysis based on density functional theory (DFT). It reveals that H absorption on different Fe sites leads to a dramatic change in magnetic coupling at FM/AFM interfaces. The interface magnetic coupling can be FMI-2 ($\downarrow$ / $\downarrow\uparrow$) when H is inserted above the Fe_3 and Fe_6 ions whereas it is FMI-1 ($\uparrow$ / $\downarrow\uparrow$) when H is located below Te5 and above Te4 ions, leading to a crossover between positive and negative EB effects. Our experiments provide evidence of possible AFM phase in vdW ferromagnet FGaT nanoflakes.

FGaT crystals with hexagonal structure of space-group $P6_3/mmc$ ($a = b = 3.986$ Å, $c = 16.229$ Å) were grown by

*These authors contributed equally to this paper.
†Corresponding author: zhaoyj@scut.edu.cn
‡Corresponding author: hxchang@hust.edu.cn
§Corresponding author: glzheng@hmfl.ac.cn

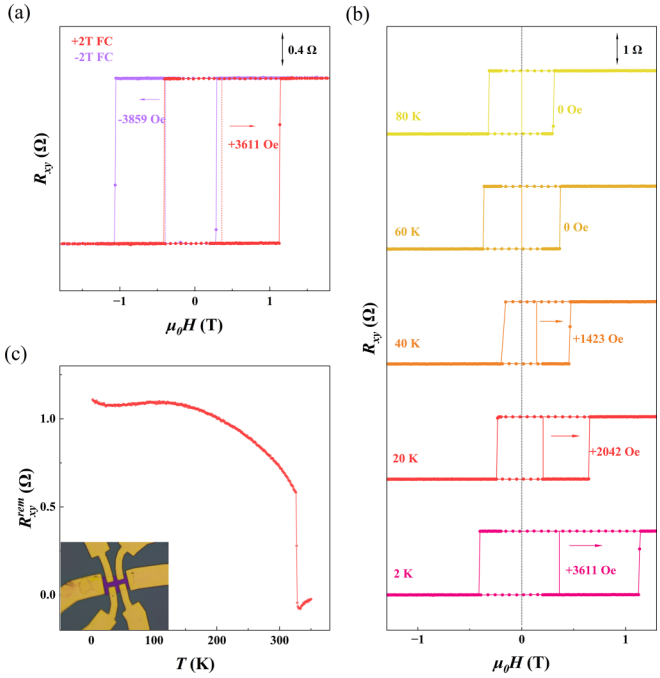

FIG. 1. (a) FC EB effects in intrinsic FGaT nanoflake (device No. 1 with thickness 17 nm) on SiO_2 after ±2 T field cooling from 200 to 2 K, respectively. (b) Temperature dependence of the FC EB effect in device No. 1 after +2-T field cooling. (c) Remanent Hall resistance R_{xy}^{rem} as a function of temperature exhibits a dip between 20 and 100 K, revealing the possible existence of the AFM phase. The inset: optical image of the FGaT Hall-bar device.

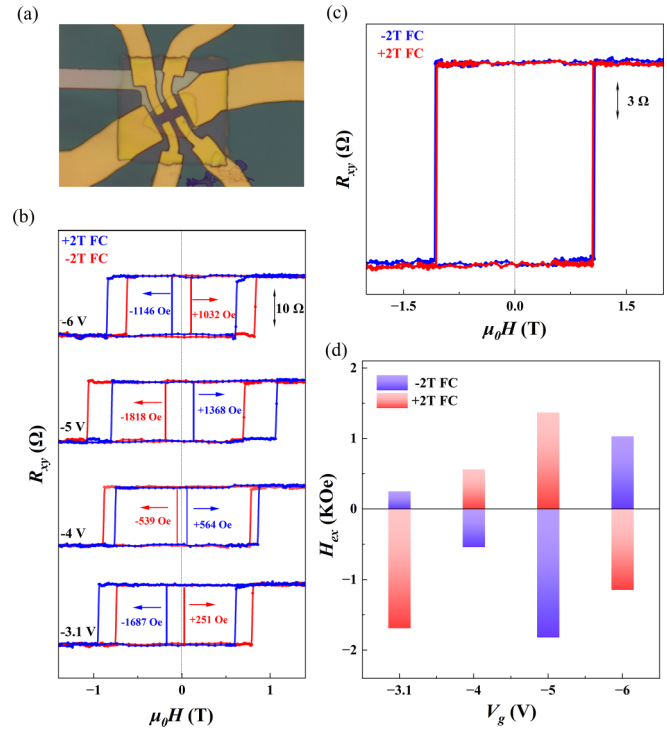

FIG. 2. (a) Optical image of one of the SP-FETs. (b) Gate dependence of the FC EB effects after ±2-T field cooling from 200 to 2 K in device No. 3 (16 nm). It clearly exhibits sign-tunable EB effects at 2 K under different gate voltages. (c) FC EB effects disappeared at $V_g = -8$ V at 2 K. (d) A summary of gate-dependent EB fields the H_{EB} in device No. 3 at 2 K.

the self-flux method as discussed in our previous study [23]. Monolayer FGaT contains two Te layers separated by the Fe_3Ga slab, and the interlayer spacing among different layers is around 0.78 nm. The large interlayer spacing allows us to get the thin FGaT nanoflakes by mechanical exfoliation. Figure 1(a) illustrates the anomalous Hall effect of a typical FGaT nanoflake (device No. 1 on SiO_2 substrate) with thickness around 17 nm at 2 K. As we can see, FGaT exhibits a much larger coercive field $H_c = (H_c^+ - H_c^-)/2$ of around 0.8 T, compared to the Fe_3GeTe_2 nanoflake at the same thickness at 2 K [24]. Generally, coercivity in ferromagnets without defects is mainly determined by the magnetic anisotropic energy, the large coercive field in FGaT reveals large perpendicular magnetic anisotropy [23].

Note that, the hysteresis loop exhibits obvious ZFC EB effect with maximal EB field $H_{EB} = 1120$ Oe at low temperatures as shown in Fig. S2 in the Supplemental Material (SM) [25]. Applying a magnetic field of 2 T (−2T) at 200 K followed by field cooling from 200 to 2 K, device No. 1 exhibits a huge positive exchange bias effect with EB field $H_{EB} =$ +3611 Oe (−3859 Oe) as shown in Fig. 1(a). Figure 1(b) illustrates the temperature-dependent EB effects with a cooling field of 2 T, and the FC EB disappears at around 60 K. The intrinsic EB effects in FeGaT nanoflakes on SiO_2 substrates are further confirmed in device No. 2 in Fig. S3 of the Supplemental Material [25]. Interestingly, we find the FC EB effect in FGaT nanoflakes can be either positive or negative, but the sign of the EB effects remains unchanged after multiple field coolings as we can see in Fig. S4 in the SM [25]. Generally, EB effect arises in different types of magnetic interfaces, such as FM-antiferromagnetic (AFM) [26], FM-ferrimagnetic [27], and AFM-ferrimagnetic [28] interfaces. In ion-based van der Waals ferromagnets Fe_3GeTe_2, the coexistence of FM and AFM phases is confirmed recently by the observation of EB effects [19]. It is possible that similar AFM phases are formed in FGaT nanoflakes. To clarify this point, we first saturated the Hall resistance R_{xy} with ±2 T at 2 K, the field was then reduced to zero, and the temperature-dependent zero-field Hall resistance $R_{xy}^{\pm}$ was examined. The temperature-dependent remnant Hall resistance $R_{xy}^{rem} = (R_{xy}^{+} - R_{xy}^{-})/2$ in device No. 1 is shown in Fig. 1(c). As we can see, the $R_{xy}^{rem} - T$ curve exhibits a dip between 20 and 100 K, probably due to the coexistence of AFM and FM phases in FGaT. Note that the interlayer magnetic coupling in FGaT is highly dependent on charge doping (Supplemental Material [25]). The AFM phase can be developed in FGaT due to the defects- (e.g., Fe defect-) induced charge doping.

In order to investigate the impact of proton doping on EB effects in FGaT nanoflakes, we fabricated solid proton-field effect transistor (SP-FET) [19,29]. Figure 2(a) shows one of our SP-FETs. In our SP-FET, the FGaT nanoflake was transferred onto the solid proton conductor with a Pt electrode underneath, the Hall-bar devices were then prepared by standard electron-beam lithography method. Gate voltage was applied between the Pt electrode and the source at 250 K. Generally, the protons can be stabilized once the temperature is decreased down to below 200 K.

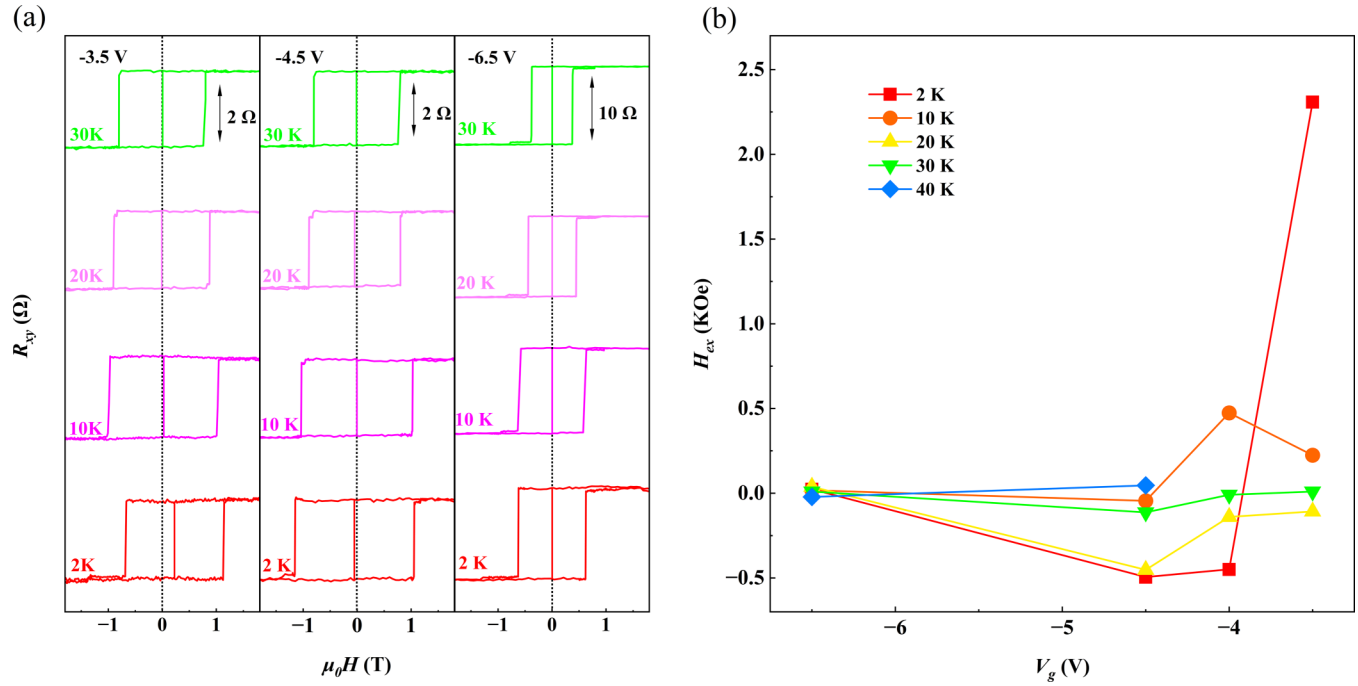

FIG. 3. (a) Gate-dependent ZFC EB effects in device No. 4 (with thickness 38 nm) at low temperatures. ZFC EB effects were totally suppressed at $V_g = -6.5$ V. (b) The corresponding gate-dependent EB field H_{EB} under different temperatures.

Figure 2(b) illustrates the gate-dependent EB effects after ±2-T field cooling from 200 to 2 K in device No. 3 (around 16 nm) on solid proton conductor. Interestingly, we observed the sign-tunable EB effects under different protonic gate voltages at 2 K. Specifically, a standard negative EB effect with $H_{EB} = -1687$ Oe (+251 Oe) was identified at $V_g = -3.1$ V after 2-T (−2-T) field cooling. However, a positive EB effect with $H_{EB} = +564$ Oe (−539 Oe) suddenly emerged after 2-T (−2-T) field cooling at $V_g = -4$ V. The EB field of the positive EB effect was further increased to $H_{EB} = +1368$ Oe (−1818 Oe) after field cooling at $V_g = -5$ V. Sweeping the gate voltage up to −6 V followed by 2-T (−2-T) field cooling, however, we found the sign of EB effect was changed back to negative again with EB field $H_{EB} = -1146$ Oe (+1032 Oe) as shown in Fig. 2(b). Interestingly, the EB effects disappeared whereas $V_g \leqslant -7$ V, this can be seen in Fig. 2(c) with $V_g = -8$ V (also in Fig. S5 in the Supplemental Material [25]). Figure 2(d) further summarized the gate-dependent EB fields H_{EB} in device No. 3. The pink bar represents 2-T field cooling whereas the purple bar represents the −2-T field cooling. It clearly shows that the EB effect can be alternatively switched to positive and negative via the protonic gate. The similar phenomenon was also observed in another device No. 4 (with thickness ∼38 nm) (see Fig. S6 in the Supplemental Material [25]). Basically, the FM/AFM interface has two different magnetic coupling types, FMI-1 (↑ / ↓↑) or FMI-2 (↓ / ↓↑) as mentioned above. If the interface coupling is FMI-1 (FMI-2), the resultant EB effect is positive (negative). The sign change in the EB effects indicates the crossover between two different magnetic coupling types at AFM/FM interfaces under different gate voltages.

Besides of the field-cooling EB effects, the ZFC EB effects can also be dramatically tuned by the protonic gate. Figure 3(a) shows the gate-dependent ZFC EB effects at different temperatures in device No. 4. At $V_g = -3.5$ V, a very large ZFC EB effect with $H_{EB} = 2308$ Oe was observed at 2 K. Increasing the temperature, we found the sign of H_{EB} was reversed, and the amplitude was largely suppressed and finally disappeared at above 30 K. Note that the coercive field $H_c = (H_c^+ - H_c^-)/2$ at 2 K is much smaller than that at 10 K. Basically, the emergence of ZFC EB with both positive and negative H_{EB} indicates that the unidirectional magnetic anisotropy occurs between the FM and the AFM domains and the magnetic coupling at AFM/FM interfaces can be both FMI-1 (↑ / ↓↑) or FMI-2 (↓ / ↓↑). We hypothesize that the energy discrepancy between these two magnetic coupling types at AFM/FM interfaces is small, and this is also consistent with our experimental observations that the intrinsic FC EB effects in different FGaT nanoflakes can be either positive or negative as discussed above. Thus, under the external perturbations, such as magnetic field and thermal fluctuation, it is possible that the magnetic coupling at AFM/FM interfaces can be transferred between FMI-1 (↑ / ↓↑) or FMI-2 (↓ / ↓↑) even in a single hysteresis loop [19]. Under this circumstance, the coercive field H_c can be increased or decreased in the ZFC EB effect, depending on the type and magnitude of the magnetic coupling at the AFM/FM interfaces. Similar phenomena were also observed at $V_g = -4$ V. Sweeping the gate voltage to −6.5 V, however, the ZFC EB effects disappeared. Besides of the gate-tunable EB effect, we found both the coercive field and the anomalous Hall resistivity can also be largely tuned. We take $T = 30$ K (with negligible EB effects), for example, both coercive field (with $H_c = 0.8$ T) and anomalous Hall resistance (with $R_{xy}^{AHE} = 1.4$ Ω) are nearly unchanged at −3.5 and −4.5 V. At − 6.5 V, however, H_c decreases to 0.38 T whereas R_{xy}^{AHE} increases up to 6.5 Ω. Those dramatic changes highlight possible gate-tuned anomalous Hall effect and magnetic anisotropy at above room temperatures in FGaT.

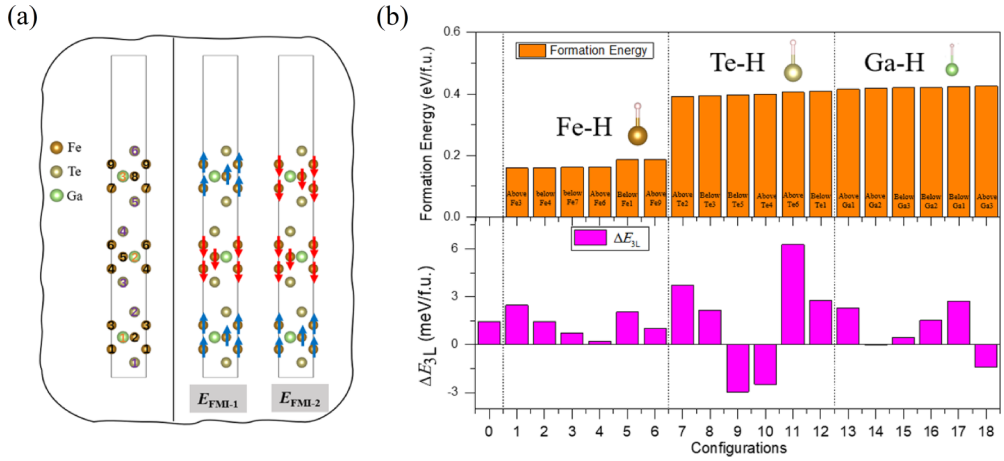

FIG. 4. (a) The illustration of structural and magnetic configurations of Fe_3GaTe_2. (b) The calculated formation energy and $\Delta E_{(3L)}$ with various *H*-inserting sites. Here, the structural configurations were sorted by the formation energy.

Figure 3(b) summarized the ZFC EB effects under different gate voltages and temperatures, and ZFC EB effects only survive at low temperatures with $V_g > -6.5$ V.

To understand those observations, we conducted the theoretical studies based on the DFT [30,31]. The constructed FM/AFM Fe_3GaTe_2 interface is shown in Fig. 4(a). According to the Malozemoff random field mode [32–34], the EB effect can be estimated by $H_{EB} = \Delta E_{3L}/2M_F t_F$ with M_F and t_F being the magnetization and thickness of the ferromagnet, respectively. ΔE_{3L} is the energy difference between two different magnetic configurations FMI-1 ($\uparrow$ / $\downarrow\uparrow$) or FMI-2 ($\downarrow$ / $\downarrow\uparrow$). Therefore, the exchange bias strongly depends on the FM/AFM interface magnetic coupling [32], and its intensity can be characterized by the energy difference between FMI-1 ($\uparrow$ / $\downarrow\uparrow$) or FMI-2 ($\downarrow$ / $\downarrow\uparrow$). Figure 4(b) presents the formation energy (H_F) and ΔE_{3L} with various H-inserting sites. H locates around Fe ions are more energetically favorable as the H_F of Fe sites are lower than that of Ga and Te sites (the origin bar diagram). Regarding the Fe sites, ΔE_{3L} reaches the maximum and minimum values when H is inserted above the Fe_3 and Fe_6 ions. The extreme values can be explained by the compensation theory [32]. H can reduce the magnetic moment of the neighboring Fe ion [Figure S11(a) in the Supplemental Material [25]; see, also, Refs. [35–40] therein], leading to an unbalanced interface magnetic coupling. For example, H absorbed above Fe_6 ion could directly weaken the AFM/FM layers coupling. Although H absorbed above the Fe_3 ion could decrease the magnetic coupling of the bottom two layers and, consequently, enhance the coupling of AFM/FM interface. If a large voltage is applied, the concentration of H increases and continues to occupy the sites with higher formation energy, i.e., sites around Te and Ga ions. ΔE_{3L} even presents negative values when H is located below Te5 and above Te4 ions, indicating the observed sign change in the EB effect. This may be ascribed to the redistribution of interface charge due to H insertion as plotted in Fig. S12 in the Supplemental Material [25] (see, also, Refs. [35–40] therein). As for the insertion near Ga, ΔE_{3L} presents complicated results since its value relies on the different absorbing sites. Note that ΔE_{3L} can also be extremely small when H locates at above Fe_6 and above Ga_2. This probably explains the disappearance of EB effects under the protonic gate since $H_{EB} = \Delta E_{3L}/2M_F t_F$.

In conclusion, we observed both FC and ZFC EB effects in above-room-temperature vdW ferromagnet Fe_3GaTe_2 nanoflakes. Applying a protonic gate, we found both amplitude and sign of magnetic coupling (ΔE_{3L}) at FM/AFM interface can be dramatically tuned by gate-induced proton intercalation, giving rise to sign-tunable EB effects in Fe_3GaTe_2 nanoflakes. The intrinsic huge EB effect and its tunability promise more applicable room-temperature vdW spintronic devices.

This work was supported by the National Key R&D Program of the MOST of China (Grants No. 2022YFA1602603 and No. 2022YFE0134600), the Natural Science Foundation of China (Grants No. 12274413, No. U19A2093, No. 12074126, No. 52272152, No. U2032164 and No. 12174394), Collaborative Innovation Program of Hefei Science Center, CAS (Grant No. 2022HSC-CIP017) and the Foundation for Innovative Research Groups of the National Natural Science Foundation of China (Grant No. 51621001).

[1] B. Huang *et al.*, Nature (London) **546**, 270 (2017).
[2] C. Gong *et al.*, Nature (London) **546**, 265 (2017).
[3] Z. Fei, B. Huang *et al.*, Nature Mater. **17**. 778 (2018).
[4] M. Gibertini *et al.*, Nat. Nanotechnol. **14**, 408 (2019).
[5] Y. Deng *et al.*, Nature (London) **563**, 94 (2018).
[6] A. F. May *et al.*, ACS Nano. **13**, 4436 (2019).
[7] J. Seo, D. Y. Kim *et al.*, Sci. Adv. **6**, eaay8912 (2020).
[8] T. Song *et al.*, Science **360**, 1214 (2018).
[9] D. R. Klein *et al.*, Science **360**, 1218 (2018).
[10] S. Jiang, J. Shan, and K. F. Mak, Nature Mater. **17**. 406 (2018).
[11] B. Huang *et al.*, Nat. Nanotechnol. **13**, 544 (2018).

[12] S. Jiang, L. Li, Z. Wang, K. F. Mak, and J. Shan, Nat. Nanotechnol. **13**, 549 (2018).
[13] Z. Wang, T. Zhang *et al.*, Nat. Nanotechnol. **13**, 554 (2018).
[14] Z. Wang *et al.*, Nat. Commun. **9**, 2516 (2018).
[15] Z. Wang, M. Gibertini *et al.*, Nat. Nanotechnol. **14**, 1116 (2019).
[16] H. H. Kim *et al.*, Proc. Natl. Acad. Sci. USA **116**, 11131 (2019).
[17] X. Wang *et al.*, Sci. Adv. **5**, eaaw8904 (2019).
[18] S. Albarakati *et al.*, Sci. Adv. **5**, eaaw0409 (2019).
[19] G. Zheng *et al.*, Phys. Rev. Lett. **125**, 047202 (2020).
[20] W. Zhuo *et al.*, Adv. Mater. **33**, 2008586 (2021).
[21] L. Meng *et al.*, Nat. Commun. **12**, 809 (2021).
[22] E. J. Telford *et al.*, Nature Mater. **21**, 754 (2022).
[23] G. Zhang *et al.*, Nat. Commun. **13**, 5067 (2022).
[24] C. Tan *et al.*, Nat. Commun. **9**, 1554 (2018).
[25] See Supplemental Material at http://link.aps.org/supplemental/10.1103/PhysRevB.107.L140409 for further information about extended experimental data and theoretical analysis.
[26] W. H. Meiklejohn and C. P. Bean, Phys. Rev. **102**, 1413 (1956).
[27] W. C. Cain and M. H. Kryder, J. Appl. Phys. **67**, 5722 (1990).
[28] G. Salazar-Alvarez, J. Sort, S. Suriñach, M. D. Baró, and J. Nogu´es, J. Am. Chem. Soc. **129**, 9102 (2007).
[29] G. Zheng *et al.*, Nat. Commun. **12**, 3639 (2021).
[30] P. Hohenberg and W. Kohn, Phys. Rev. **136**, B864 (1964).
[31] W. Kohn and L. J. Sham, Phys. Rev. **140**, A1133 (1965).
[32] A. P. Malozemoff, Phys. Rev. B **35**, 3679 (1987).
[33] A. P. Malozemoff, J. Appl. Phys. **63**, 3874 (1988).
[34] A. P. Malozemoff, Phys. Rev. B. **37**, 7673 (1988).
[35] J. Hafner, J. Comput. Chem. **29**, 2044 (2008).
[36] P. E. Blöchl, Phys. Rev. B **50**, 17953 (1994).
[37] J. P. Perdew, K. Burke, and M. Ernzerhof, Phys. Rev. Lett. **77**, 3865 (1996).
[38] H. J. Monkhorst and J. D. Pack, Phys. Rev. B **13**, 5188 (1976).
[39] Mandl, *Statistical Physics [M].* 2nd ed. (Wiley, West Sussex, 1988).
[40] Hansen H. A., Rossmeisl J., and Nørskov J. K., Phys. Chem. Chem. Phys. **10**, 3722 (2008).